Pergamon

J. Mech. Phys. Solids, Vol. 42, No. 6, pp. 877–896, 1994

0022–5096/94 $7.00 + 0.00

0022–5096(94)E0012–S

CLEAVAGE DUE TO DISLOCATION CONFINEMENT IN LAYERED MATERIALS

K. J. HSIA

Department of Theoretical and Applied Mechanics, University of Illinois, Urbana, IL 61801-2935, U.S.A.

Z. SUO

Mechanical and Environmental Engineering Department, Materials Department, University of California, Santa Barbara, CA 93106, U.S.A.

and

W. YANG

Department of Engineering Mechanics, Tsinghua University, Beijing 100084, China

(*Received* 2 *November* 1993; *in revised form* 12 *February* 1994)

ABSTRACT

THE EFFECTS OF dislocation confinement on fracture behavior in laminates consisting of alternating submicron ductile and brittle layers are studied. When the ductile layer thickness is below the micron level, dislocations must be treated individually. Dislocations emitted from the crack tip have two effects: they blunt the crack and thereby reduce the tensile stress at the crack tip; and pile up against an interface and send a back stress to the crack tip to hinder further dislocation emission. Consequently, an equilibrium number of dislocations exists at a given load level. We estimate this number by considering the stability conditions for dislocations threading in the ductile layer, and dislocation pile-up is treated as an equivalent superdislocation. Furthermore, the competition between further dislocation emission and cleavage at the blunted crack tip is considered. Our result shows that because of the confinement, as the applied load increases, the tensile stress at the blunted crack tip also increases. Cleavage occurs when the tensile stress at the crack tip reaches the theoretical strength. Given a sufficiently thin constraining layer, cleavage can even occur in ductile metals such as copper and aluminum. The implications of this model for several material systems are discussed.

1. INTRODUCTION

MODERN materials processing technologies can control microstructures at length scales substantially smaller than traditional processing methods. Examples include layered materials with each layer ranging from 10 to 10^3 nm thick, and nano-composites or structures (LANGER, 1992). These materials may exhibit mechanical behaviors different from those in traditional materials. In this paper we study the consequences of *dislocation confinement* by narrowly spaced internal boundaries.

Consider, for example, a laminate consisting of alternating ductile and brittle layers with a pre-existing crack at an interface. Upon loading, the ductile phase flows and blunts the crack tip. If the ductile layer thickness h is sufficiently large, the flow and

blunting at the crack tip will proceed until a limiting event intervenes. Depending on the material system, such an event can be cleavage at some distance ahead of the blunted crack tip (RITCHIE *et al.*, 1973), or void growth and its linkage with the blunted crack tip (MCMEEKING, 1977). Gas pores, brittle particles and other defects on the interface supply the initiation sites for voids or microcracks. In this case, the characteristic length scale is the spacing between the defects. Fracture toughness is thus governed by the plastic dissipation of metal ligaments between voids (EVANS and DALGLEISH, 1992).

For a crack in a ductile metallic layer with large h ($h \to \infty$), the plastic zone size at the onset of fracture is

$$r_p = \frac{1}{2\pi}\left(\frac{K_c}{\sigma_Y}\right)^2, \tag{1}$$

where K_c is the fracture toughness and σ_Y the yield strength of the metal. For a typical metal such as steel, the crack tip plastic zone is of the order of millimeters to centimeters. Therefore, in a ductile layer larger than a few centimeters, no confinement exists, and the measured fracture energy is independent of layer thickness. However, the plastic flow becomes confined when $h < 2r_p$, resulting in a lower fracture energy, as shown schematically in Fig. 1. VARIAS *et al.* (1991) have shown that, because of the confinement, the tensile stress at the crack tip increases as h decreases. For a given h, the tensile stress peaks at a distance several times h ahead of the crack tip. Consequently, fracture toughness decreases as h decreases.

When h approaches the micron level, the dislocation activities within the thin ductile layer can no longer be treated with continuum plasticity theory (Fig. 1). For layer thicknesses below the length scale of a micron and down to about 10 nm, individual

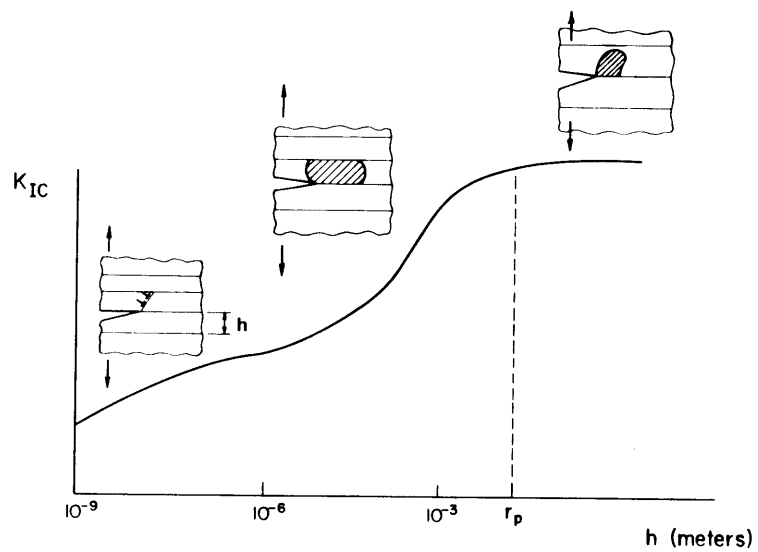

FIG. 1. Schematic illustration of the fracture energy as a function of layer thickness. Listed in the figure are also the underlying confinement situations in various thickness regimes.

dislocations interact with the crack tip and the interface. Interfaces act as barriers which prevent the dislocations from crossing over into the brittle layer. This is the regime to be studied in the present paper. Experimental data indicated that as the layer thickness decreases, the material appears increasingly more brittle, absorbing smaller amounts of energy at fracture (EVANS and DALGLEISH, 1992), even though the volume fraction of the ductile metal is substantial in these layered materials.

In this paper, we present a theoretical study on the confinement to individual dislocations in layered materials. The length scales of the confining layer thickness considered in this study are those below a few microns, thus only the effects of individual dislocations are relevant. The equilibrium number of dislocations which thread through the confining layer will be estimated from an energetic point of view. The competition between cleavage and continued dislocation threading will be evaluated. Our results indicate that confinement to dislocation motion by interfaces is very effective in reducing plastic deformation in layered materials. Cleavage may even occur in ductile metals such as aluminum and copper, provided the confining layer is sufficiently thin.

2. Dislocation Confinement Leading to Cleavage

For a layered material with a crack subjected to an applied load, as long as the ductile layer thickness is much larger than the Burgers vector, dislocations will emit and move away from the crack tip. Figure 2 shows dislocations in materials composed of alternating ductile and brittle thin layers. Cracks can be either parallel [Figs 2(a) and (b)] or perpendicular [Fig. 2(c)] to the interfaces. In the former, the crack can be either along an interface [Fig. 2(a)] or inside a ductile layer [Fig. 2(b)]. In every case, dislocations emitted from the crack tip tend to pile up against the interfaces (ANDERSON and LI, 1993). We assume that the dislocation pile-ups do not cause cracking in the brittle layer. We then investigate whether cleavage can occur in the ductile layer or along the interface, and evaluate the fracture toughness associated with such a fracture mode for various layer thicknesses.

These dislocations have two effects on the crack tip. First, if the Burgers vector has a component normal to the crack plane, the emitted dislocations blunt the crack tip. This reduces the stress concentration at the crack tip, making it more difficult to reach the cohesive tensile strength. Second, the interaction forces between the crack and the emitted dislocations will result in crack tip shielding, giving rise to a crack tip stress intensity lower than the far field applied stress intensity. In the absence of confinement, dislocations can move freely away from the crack tip. Therefore, in ductile metals such as copper and aluminum, blunting becomes substantial, and the unlimited dislocation emission sufficiently reduces the crack tip stress. Consequently, the crack tip stress cannot reach the cohesive strength and thereby cleavage is suppressed.

In a layered material, however, dislocations are confined by the brittle layers. The confined dislocations send a back stress to the crack tip which impedes further dislocation emission. For a given applied load and layer thickness, there exists an equilibrium number of dislocations in the pile-ups. Once the equilibrium number is reached, emission of additional dislocations is prevented by the back stress. It is this

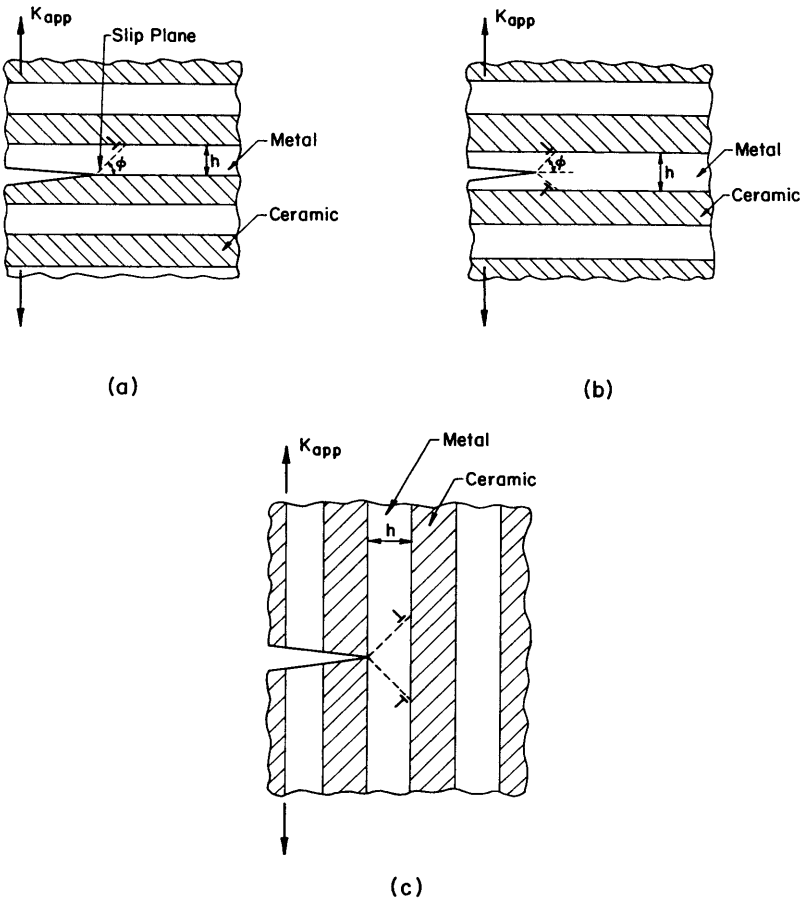

FIG. 2. Dislocation emission from a crack in layered structures. (a) A crack along the interface; (b) a crack within the ductile layer parallel to the interface; (c) a crack normal to the interface.

back stress that hinders further blunting of the crack tip. After a limited blunting, the crack tip tensile stress will gradually build up as the applied stress intensity increases. Eventually, the tensile stress at the blunted crack tip reaches the cohesive strength, leading to cleavage fracture. The fracture toughness of the material (critical far field applied stress intensity at fracture) depends on how many dislocations can be emitted from the crack tip, which in turn depends on the thickness of the ductile layer.

It was demonstrated by RICE and THOMSON (1974) that dislocations nucleate spontaneously from the crack tip in ductile metals such as aluminum and copper. Thus, only dislocation motion is considered here. We envision a specific process by which dislocations move away from the crack tip. As shown in Fig. 3, each dislocation first protrudes out from one dislocation source on the crack front. Then, when the outermost part of the protrusion reaches its equilibrium position against the existing pile-up, the dislocation moves parallel to the crack front. The details of this threading

motion are depicted in Fig. 3(b), viewed from the dislocation gliding plane. The process is similar to the dislocation threading process in epitaxial thin films (FREUND, 1987). For a given applied load, the threading of a new dislocation is prevented by the dislocation pile-up at the interface. The equilibrium number of the dislocations in the pile-up can then be estimated by the stability condition of the threading dislocations.

3. A MECHANISTIC MODEL

Consider a material with alternating brittle and ductile layers containing a crack parallel to the interface and substantially longer than the layer thickness, as shown in

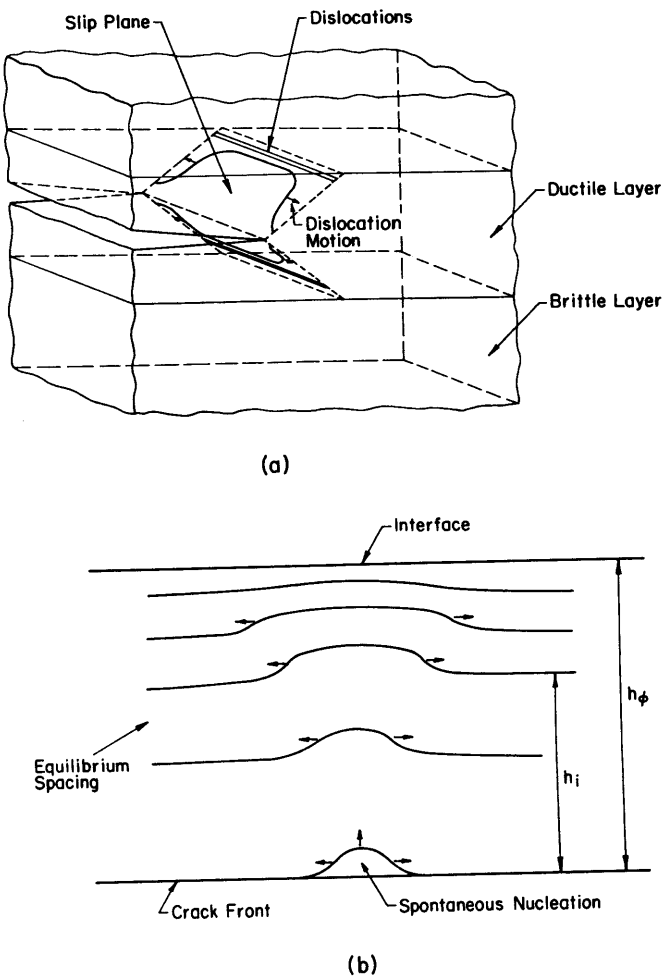

FIG. 3. Dislocations thread through the ductile layer. (a) A 3-D view; (b) projection on the glide plane for an array of threading dislocations; (c) approximation by an idealized superdislocation with the last dislocation threading through the glide plane.

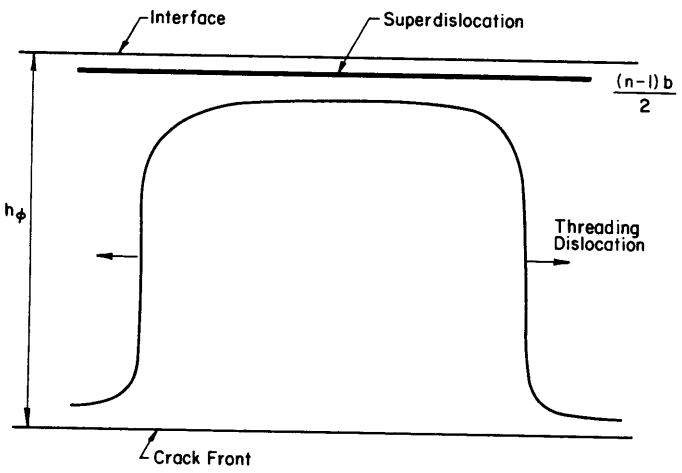

(c)

FIG. 3—*continued.*

Fig. 2(b). The thickness of the ductile metal layer is denoted by h. It is assumed that a pair of symmetric slip systems, with the slip plane inclined from the interface by an angle ϕ [marked in Fig. 2(b)] will be activated upon loading. Thus all dislocations emitted from the same crack tip source would pile up against the interfaces, and the leading ones can travel a maximum distance of $h_\phi = h/(2 \sin \phi)$ before they are blocked by the upper and lower interfaces. The applied load is represented by a far field mode I stress intensity K_{app}.

To avoid mathematical complications yet retain the essence of the confinement, the layered material is assumed to be elastically homogeneous and isotropic. This implies that the elastic crack tip field is identical to that of a homogeneous isotropic material, and the interface exerts no image forces on the dislocations. The following analysis can, however, be in principle extended to the more realistic material systems where elastic mismatch exists. Under the above assumptions, only the following material parameters are needed: shear modulus μ, Poisson's ratio ν, Burgers vector b, surface energy γ and cohesive strength σ_c. In the following formulation, these quantities will be normalized as

$$\tilde{K}_{app} = \frac{K_{app}}{\mu\sqrt{b}}, \quad \tilde{\gamma} = \frac{\gamma}{\mu b}, \quad \tilde{h} = \frac{h_\phi}{b}, \quad \tilde{\sigma} = \frac{\sigma}{\mu}, \tag{2}$$

where σ can be any characteristic stress.

3.1. *Representation of dislocation clusters—superdislocation model*

Attention is now focused on one arm of the dislocation pile-ups (consisting of $n/2$ dislocations, Fig. 3) emitted from the crack tip. Even for dislocations perfectly aligned in a single slip system, calculation for their equilibrium spacings is cumbersome.

As pointed out by LIN and THOMSON (1986), the mutual interactions between the dislocations are in general not one-dimensional. However, an analysis of minimum energy configuration of multiple dislocations by LUBARDA *et al.* (1993) demonstrates that there is a strong tendency for dislocations to form narrow bands or walls in space. Here an equivalent superdislocation consisting of a condensed pile-up with a Burgers vector $nb/2$ is suggested to circumvent this difficulty. A justification of this approximation is outlined below. If the dislocations in one arm of the pile-ups are located at

$$h_i = h_\phi - \Delta_i, \quad i = 1, \ldots, n/2, \tag{3}$$

we can then treat the dislocation cluster as a superdislocation provided that the majority of Δ_is ($i = 1, \ldots, n/2$) are much smaller than h_ϕ. The equivalent distance between the superdislocation and the crack tip will be smaller than h_ϕ. This superdislocation model is justified if the normalized layer thickness $\tilde{h}$ defined in (2) is much larger than n, the number of emitted dislocations. It is noted that the threading motion of dislocations shown in Fig. 3(b), rather than the single dislocation threading in Fig. 3(c), is more realistic. But we will show in the following that, although quantitative errors (usually less than a factor of 2) may be introduced by the approximation, qualitative features are well preserved using the superdislocation model [Fig. 3(c)].

3.2. *Equilibrium number of dislocations*

An energy approach is employed which is similar to that in the study of dislocation threading in epitaxial films by FREUND (1987). The central argument is as follows. In the presence of $(n-1)$ dislocations, if the total energy decreases by threading an additional dislocation across the whole crack front, the state with n dislocations is energetically preferable. Therefore, to determine the equilibrium number of dislocations, we need only to evaluate the energy difference between the state with $(n-1)$ dislocations and the one with n dislocations.

The total energy in the system consists of (1) the self energy of the existing dislocations, W_d, including the self energy for all individual dislocations and their interaction energy; (2) the self energy of the crack tip stress field under far field stress intensity; (3) the interaction energy between the dislocation stress field and the crack tip field, W_K; and (4) the surface energy due to creation of dislocation ledges, W_L. The self energy of the crack tip field does not change with the introduction of additional dislocations and thus will be ignored here. Moreover, the friction stress against the dislocation motion, such as Peierls–Nabarro stress, does not enter the two energy states to be compared. Therefore, the total energy of the system in the presence of two equivalent superdislocations of strength $nb/2$ can be summed as

$$W_T = W_d + W_K + W_L, \tag{4}$$

where W_d, W_K and W_L are derived in Appendix A as

$$W_d = \frac{\mu(nb)^2}{8\pi(1-\nu)}(\ln(h_\phi/r_0) - C) \tag{4a}$$

$$W_K = -\frac{K_{app}}{A\sqrt{2\pi}}\sqrt{h_\phi}(nb)\sin\phi\cos\frac{\phi}{2} \tag{4b}$$

$$W_L = (nb)\gamma. \tag{4c}$$

In (4a), C is a constant in the neighborhood of unity, and the effective core radius r_0 of the dislocation cluster is given by

$$r_0 = \left(\prod_{k=1}^{n/2}\prod_{q=1}^{n/2}\Delta_{kq}\right)^{1/(n/2)^2}, \tag{5}$$

where

$$\begin{aligned}\Delta_{kq} &= r_{crack} \quad \text{if } k = q,\\ \Delta_{kq} &= |\Delta_k - \Delta_q| \quad \text{if } k \neq q,\end{aligned} \tag{6}$$

and r_{crack} is the core radius of a dislocation at the crack tip. The factor A in (4b) is slightly greater than unity,

$$\frac{1}{A} = \frac{2}{n}\sum_{i=1}^{n/2}\sqrt{h_i/h_\phi}. \tag{7}$$

As a typical example to estimate r_0, consider 10 dislocations equally spaced over a length of $100b$, then r_0 is evaluated as $10b\times(10^{-5}\times 2^8\times 3^7\times 4^6\times 5^5\times 6^4\times 7^3\times 8^2\times 9)^{1/50} = 21.15b$. This estimate suggests that r_0 can be significantly smaller than the extended length of dislocation array. With further simplification to an idealized superdislocation located at $r = h_\phi$, r_0 reduces to the core size of a dislocation and $A = 1$.

Between the two states with superdislocation of strengths $(n+1/2)b$ and $(n-1/2)b$, the total energy of the system differs by

$$\Delta W_T = W_T((n+1/2)b) - W_T((n-1/2)b). \tag{8}$$

The following stability condition arises:

$\Delta W_T > 0 \Rightarrow$ the dislocation shrinks back to crack,

$\Delta W_T < 0 \Rightarrow$ the dislocation threads out,

$\Delta W_T = 0 \Rightarrow$ equilibrium.

From this condition, the equilibrium number of dislocations can be given as,

$$n = \frac{4\pi(1-\nu)}{\ln(\tilde{h}/\tilde{r})}\left(\frac{\tilde{K}_{app}\sqrt{\tilde{h}}}{A\sqrt{2\pi}}\sin\phi\cos\frac{\phi}{2} - \tilde{\gamma}\right), \tag{9}$$

where

$$\tilde{r} = \frac{r_0}{b}e^C \approx 2.7\frac{r_0}{b}. \tag{10}$$

For a given ductile layer thickness, the equilibrium number of dislocations increases

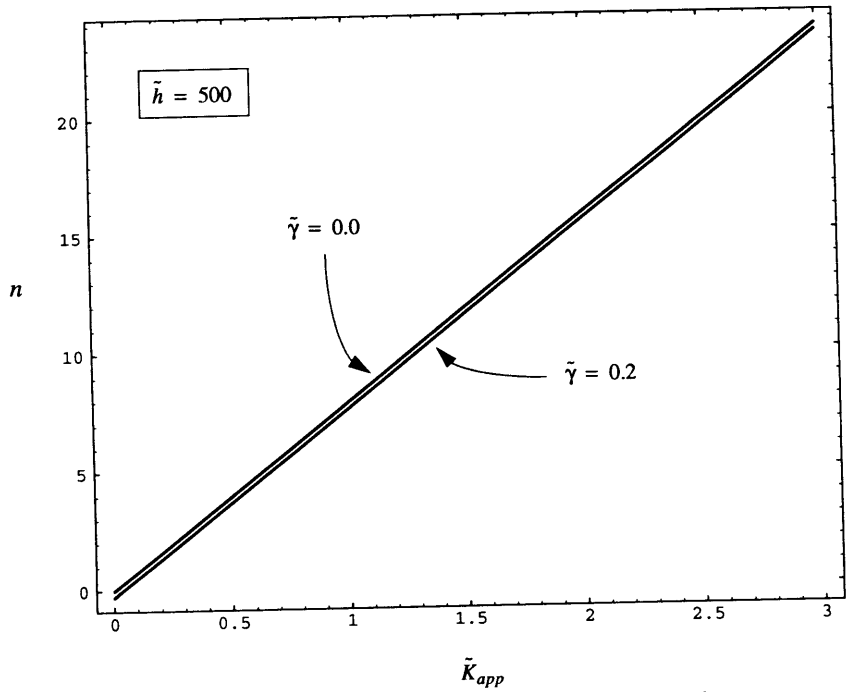

Fig. 4. The equilibrium number of dislocations n vs applied stress intensity $\tilde{K}_{app}$ for $\tilde{h} = 500$, $\tilde{\gamma} = 0$ and 0.2.

linearly with the applied stress intensity. Figure 4 shows n as a function of $\tilde{K}_{app}$ for two values of $\tilde{\gamma}$. Unless otherwise specified, we take $\tilde{r} = 1$, $A = 1$ (an idealized superdislocation), $\phi = 45°$, and $\nu = 0.33$ in all the drawings. In Fig. 4, a fixed ductile layer thickness $\tilde{h} = 500$ ($h_\phi = 500b$) is chosen. The values of $\tilde{\gamma}$ for a few ductile metals have been estimated by RICE and THOMSON (1974) as Cu: 0.1684; Au: 0.2085; Al: 0.1174. Here we choose two limiting cases of $\tilde{\gamma} = 0$ and $\tilde{\gamma} = 0.2$. The results show that the equilibrium number of dislocations is insensitive to surface energy since the values of surface energy of different materials do not differ appreciably. As the value of surface energy increases, the number of dislocations decreases slightly.

The effect of ductile layer thickness is to change the slope of the n versus $\tilde{K}_{app}$ curve, as shown in Fig. 5. The thicker the ductile layer, the more the emitted dislocations at a given $\tilde{K}_{app}$. For all the cases considered here, the equilibrium number of dislocations emitted from the crack tip is fairly small.

A more accurate approximation of the equivalent superdislocation infers an $\tilde{r}$ value greater than one, which increases the equilibrium number of dislocations by a factor of

$$f = \frac{1}{1 - \ln \tilde{r}/\ln \tilde{h}} \geqslant 1. \tag{11}$$

One can readily use the curves furnished in Figs 4 and 5, and multiply them by this

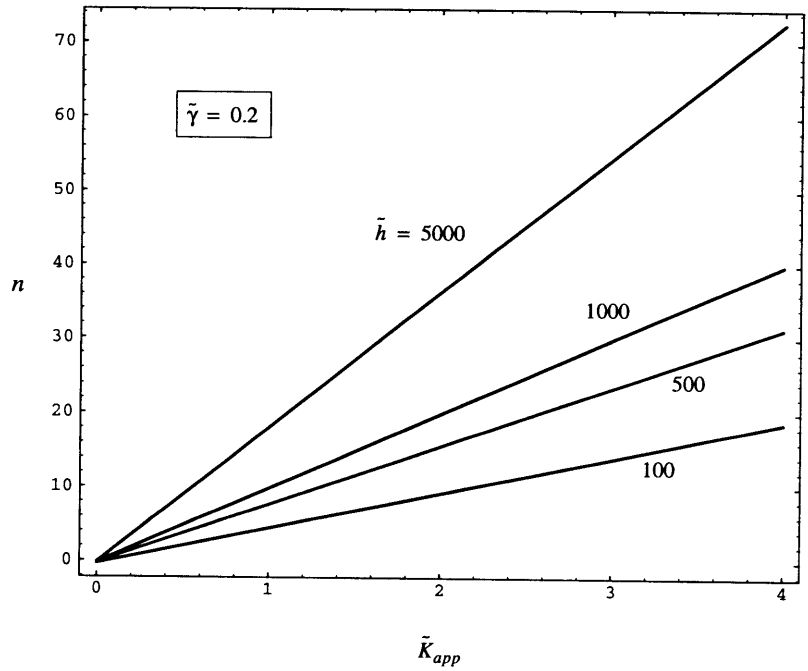

FIG. 5. Influence of layer thickness on n vs $\tilde{K}_{app}$ curve, $\tilde{h} = 100$, 500, 1000, 5000 and $\tilde{\gamma} = 0.2$.

factor to assess more accurately the equilibrium number of dislocations. The influence of A on such a prediction is commonly small because the value of A is only slightly larger than unity. Therefore, the idealized superdislocation case used in plotting Figs 4 and 5 moderately underestimates the equilibrium number of dislocations. For $\tilde{h} = 1000$, the underestimation is one third if $\tilde{r} = 10$. For $\tilde{h} = 10{,}000$, the underestimation is one fourth if $\tilde{r} = 10$ and one half if $\tilde{r} = 100$.

3.3. *Crack tip analysis*

The interactions between a crack tip and a dislocation have been extensively studied (e.g. LIN and THOMSON, 1986) in terms of the image force on the dislocation. A shielding dislocation reduces the crack tip stress intensity, whereas an anti-shielding dislocation increases the crack tip stress intensity. In the presence of a shielding dislocation, the crack tip stress intensity is

$$K_{tip} = K_{app} - K_D. \tag{12}$$

Here K_D is the contribution of the dislocation to the crack tip stress intensity (LIN and THOMSON, 1986):

$$K_D = \frac{\mu b}{(1-\nu)\sqrt{2\pi h_\phi}} \frac{3}{2} \sin\phi \cos\frac{\phi}{2} \tag{13}$$

for a dislocation located at the interface. The crack tip stress intensity in the presence of a pair of equivalent superdislocations of strength $nb/2$ is

$$K_{tip} = K_{app} - \frac{A\mu(nb)}{(1-\nu)\sqrt{2\pi h_\phi}} \frac{3}{2} \sin\phi \cos\frac{\phi}{2}. \tag{14}$$

Here the meaning of A as an amplification factor for shielding becomes evident.

The second effect of the emitted dislocations is to create ledges at the crack tip. The blunting due to these ledges reduces the maximum tensile stress ahead of the crack tip. For simplicity, we approximate the blunted crack tip by a notch with tip radius $nb/2$, as shown in Fig. 6. The notch tip maximum tensile stress is

$$\sigma_{tip} = \beta \frac{K_{tip}}{\sqrt{nb}}, \tag{15}$$

where $\beta = 2\sqrt{2/\pi}$ for a notch with semi-circular front (TADA *et al.*, 1985). Substituting equations (14) and (9) into (15), we obtain the maximum tensile stress at the blunted crack tip,

$$\tilde{\sigma}_{tip}\sqrt{n} = \beta\tilde{K}_{app}\left(1 - \frac{3\left(\sin\phi\cos\frac{\phi}{2}\right)^2}{\ln(\tilde{h}/\tilde{r})}\right) + \frac{3A\beta\sqrt{2\pi}}{\sqrt{\tilde{h}}\ln(\tilde{h}/\tilde{r})}\tilde{\gamma}\sin\phi\cos\frac{\phi}{2}. \tag{16}$$

For a given ductile layer thickness $\tilde{h}$, since n is proportional to $\tilde{K}_{app}$ as predicted by

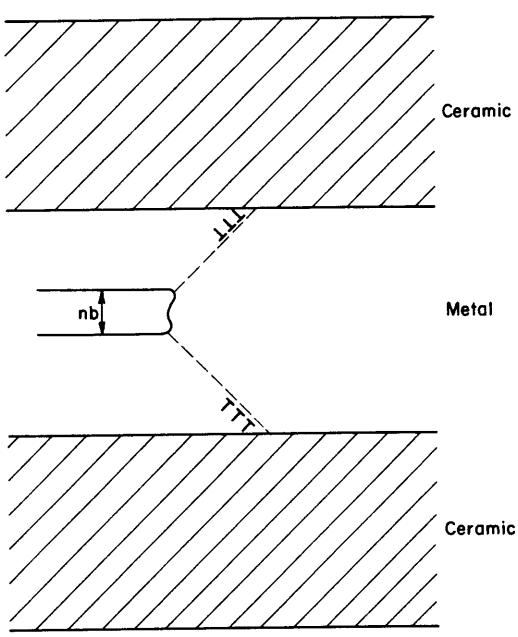

FIG. 6. Schematics of the crack tip configuration after emitting n dislocations.

(9) and $\tilde{\gamma}$ is usually small, the notch tip stress $\tilde{\sigma}_{tip}$ is roughly proportional to $\sqrt{\tilde{K}_{app}}$. This yields an important conclusion: as long as the layer thickness is small (less than a few microns), the notch tip stress will always increase with the applied loading, regardless of how ductile the layer is, or how readily a dislocation emits from the crack tip in the absence of confinement.

The normalized notch tip stress is plotted in Fig. 7 as a function of the applied stress intensity. For a given ductile layer thickness, the stress $\tilde{\sigma}_{tip}$ increases with the applied stress intensity. For very thin ductile layers, the crack tip stress can reach a considerable fraction of the shear modulus. On the other hand, a thicker ductile layer allows more dislocations to emit from the crack tip, resulting in a lower maximum tensile stress. The notch tip stress would scale down from the values in Fig. 7 by a factor of about $f^{-1/2}$ when a more accurate equivalent superdislocation is considered.

3.4. *Competition between cleavage and dislocation emission*

In a ductile metal such as Cu or Au, in the absence of the confinement, the crack tip tensile stress never reaches the cohesive strength because of easy dislocation emission and high dislocation mobility. With the confinement, however, the back stress sent by the confined dislocations tends to build up the tensile stress at the crack

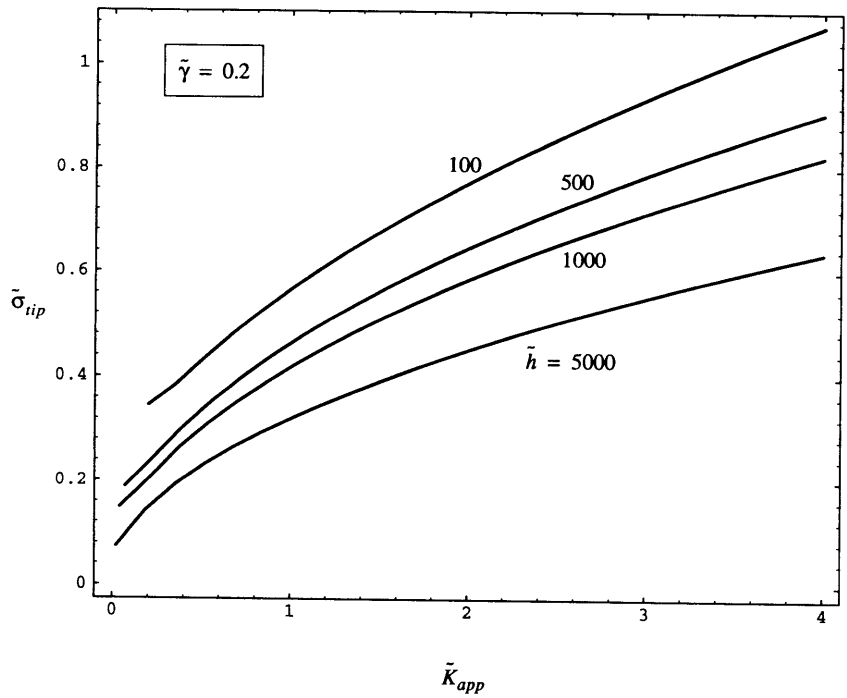

FIG. 7. Normalized notch tip stress vs $\tilde{K}_{app}$ for $\tilde{h}$ = 100, 500, 1000, 5000 and $\tilde{\gamma}$ = 0.2.

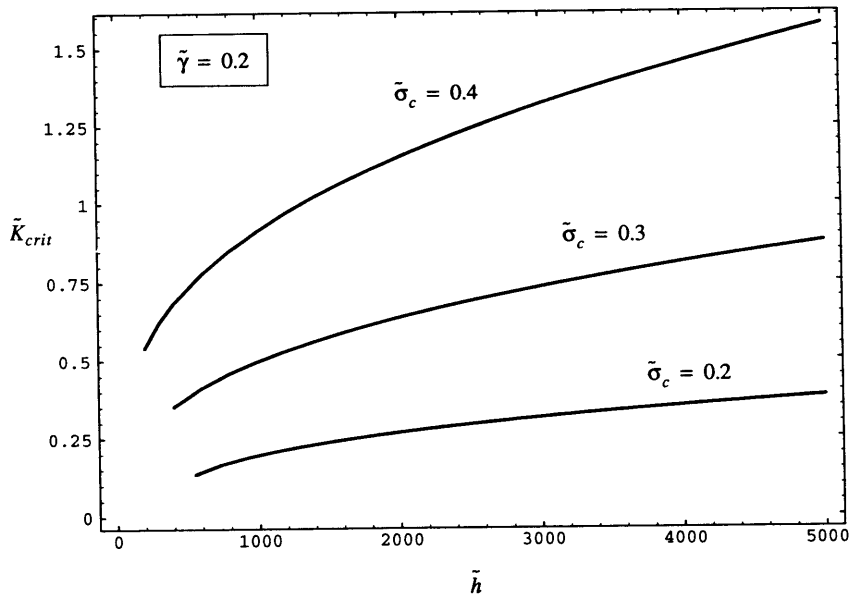

FIG. 8. Fracture toughness predicted by the current model as a function of layer thickness, $\sigma_c/\mu = 0.2$, 0.3 and 0.4, $\tilde{\gamma} = 0.2$.

tip, as indicated by (16). As the applied stress intensity increases, a competition is set up at the blunted crack tip between cleavage and continued dislocation emission.

When the crack tip tensile stress σ_{tip} reaches the cohesive strength of the material, σ_c, namely

$$\sigma_{tip} = \sigma_c, \tag{17}$$

cleavage occurs in the ductile metal layer. The far field applied stress intensity under this condition is then the fracture toughness of the layered material. Imposing condition (17) yields an expression for the fracture toughness, $\tilde{K}_{crit}$, as a function of layer thickness, which is the very relation we are trying to deduce from this model.

Figure 8 shows the fracture toughness of the layered material, $\tilde{K}_{crit}$, as a function of layer thickness inferred by an idealized superdislocation, where normalized surface energy $\tilde{\gamma} = 0.2$ and the normalized cohesive strength $\tilde{\sigma}_c = \sigma_c/\mu = 0.2$, 0.3, 0.4. Values of the normalized intrinsic fracture toughness, $\tilde{K}_{intrinsic}$, for a number of materials are given in Table 1, where intrinsic toughnesses are estimated using the data on surface energy, shear modulus and Burgers vector given by RICE and THOMSON (1974). The

TABLE 1. *Normalized intrinsic fracture toughness* $\tilde{K}_{intrinsic}$

FCC crystals			BCC crystals		Diamond cubic	
Cu	Au	Al	Fe	W	Si	C
0.98	1.19	0.85	0.80	0.46	0.51	0.43

values of the normalized intrinsic toughness range from about 0.4 for diamond cubic crystals to about 1.2 for FCC metals. It is noted from Fig. 8 that the apparent fracture toughness $\tilde{K}_{crit}$ could be very close to the intrinsic toughness when $\tilde{h}$ is small (note also that normalized cohesive strength σ_c/μ is different for different materials, and tends to be higher for FCC metals and lower for covalently bonded materials).

Figure 8 also shows that the toughness changes rapidly when the layer thickness is small, suggesting a strong effect of layer thickness on dislocation confinement. When the layer thickness is large (of the order of a micron), the fracture toughness starts to level off, indicating the curtailment of dislocation confinement effect. Figure 8 demonstrates that fracture toughness of the layered materials is rather sensitive to the cohesive strength of the ductile layer. An increase of the normalized cohesive strength from 0.2 to 0.3 causes the fracture toughness to be more than doubled. For a more realistic equivalent superdislocation, the general trend demonstrated in Fig. 8 is preserved. Quantitatively, the values of $\tilde{K}_{crit}$ should be identical to that in Fig. 8 when the layer thickness $\tilde{h}$ is small, but would be larger than that in Fig. 8 as $\tilde{h}$ increases. The level of increase depends on the layer thickness in a rather complicated way, due to the fact that the effective core size, $\tilde{r}$, is also related to $\tilde{h}$.

A special (but still very reasonable) case can be studied easily as follows. When the contribution from surface energy $\tilde{\gamma}$ is negligible, the fracture toughness can easily be solved in terms of ductile layer thickness, as

$$\tilde{K}_{crit} = \frac{C_1 \tilde{\sigma}_c^2 \sqrt{\tilde{h}}}{\beta^2 A \ln(\tilde{h}/\tilde{r}) \left[1 - \dfrac{C_2}{\ln(\tilde{h}/\tilde{r})}\right]^2}, \tag{18}$$

where C_1 and C_2 are constants determined from (9) and (16), as

$$C_1 = 2\sqrt{2\pi}(1-\nu) \sin\phi \cos\frac{\phi}{2}, \tag{18a}$$

$$C_2 = 3\left(\sin\phi \cos\frac{\phi}{2}\right)^2. \tag{18b}$$

Equation (18) gives a general trend of fracture toughness versus ductile layer thickness. It shows that $\tilde{K}_{crit}$ is proportional to $\tilde{\sigma}_c^2$, which explains why fracture toughness is so sensitive to $\tilde{\sigma}_c$ in Fig. 8. Furthermore, when the ductile layer thickness is large, $\tilde{K}_{crit}$ is proportional to $\sqrt{\tilde{h}}/\ln(\tilde{h}/\tilde{r})$. So the fracture toughness curve bends over with a rate slightly slower than $\sqrt{\tilde{h}}$ as $\tilde{h}$ approaches infinity.

4. Discussion

Our model is based on the assumption that dislocations have to be dealt with individually when the ductile layer is very thin. This assumption must be justified by

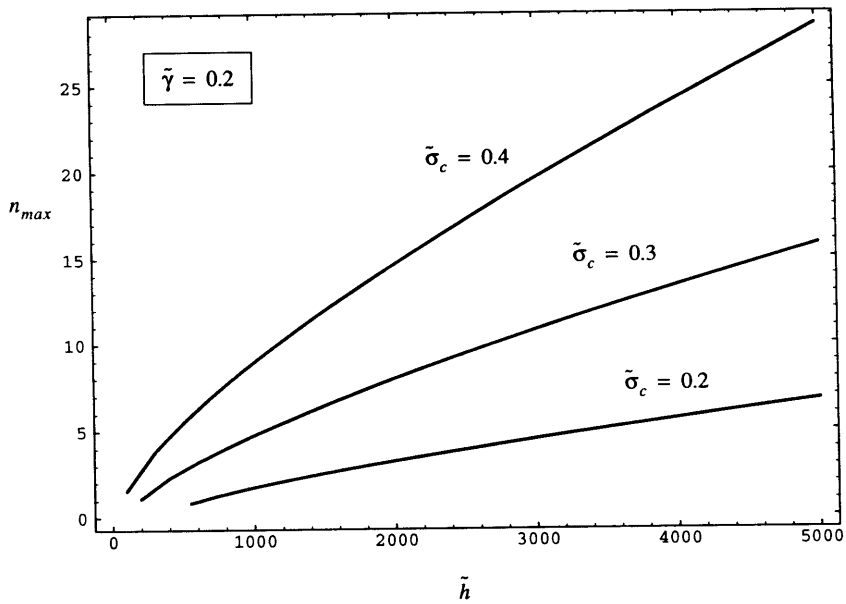

FIG. 9. Maximum number of dislocations emitted from the crack tip prior to cleavage vs ductile layer thickness, $\sigma_c/\mu = 0.2$, 0.3 and 0.4, $\tilde{\gamma} = 0.2$.

the model prediction. Figure 9 shows the maximum number of dislocations emitted from the crack front, $n_{\max}$, when the cleavage condition is achieved. The calculation is performed for an idealized superdislocation located at the interface, and the parameters used in Fig. 9 are $\tilde{\gamma} = 0.2$ and cohesive strength $\tilde{\sigma}_c = 0.2$, 0.3, 0.4. It is seen that even when the ductile layer thickness is about a few thousand Burgers vectors, the total number of emitted dislocations when cleavage fracture occurs is less than 30. Therefore, indeed, a continuum plasticity approach to this problem would be inappropriate.

With the idealized superdislocation, all dislocations are forced to be packed at the interface, which underestimates the effects of dislocation shielding and the notch tip stress for a fixed number of emitted dislocations. Consequently, in real materials, cleavage fracture in ductile layer could occur at an applied stress intensity level equal to or higher than the values predicted in Fig. 8, as one may envisage from the sizable difference between the intrinsic fracture toughness and the experimentally measured fracture toughness. Nevertheless, based on our model prediction, the toughening resulting from the limited dislocation emission would increase the critical stress intensity by only a factor of 3–8 so long as the layer thickness is smaller than a micron, a significantly smaller increase than that due to unconfined plastic flow.

The equilibrium position of dislocations can be estimated using the solution of LIN and THOMSON (1986). We estimate the order of magnitude of the equilibrium spacing by considering the first two dislocations. If the leading dislocation is blocked at the interface, the second dislocation is subjected to two forces, one from the crack tip

field, the other from the first dislocation. We neglect the lattice friction and assume the separation of the two dislocations is much smaller than h_ϕ so that the short range crack tip image force can be omitted. The balance of these forces then determines the equilibrium spacing. From a simple calculation given in Appendix B, the equilibrium spacing of the first two dislocations is obtained as,

$$r_e = \frac{b}{S}[\sqrt{1+2S\tilde{h}}-1], \tag{19}$$

where S, the strength of the applied field, is given by,

$$S = \pi(1-\nu)^2 \sin^2\phi \cos^2\frac{\phi}{2}\tilde{K}_{app}^2. \tag{20}$$

For materials with $\tilde{\gamma} = 0.2$ and $\tilde{\sigma}_c = 0.3$, the equilibrium spacing r_e at $\tilde{K}_{app} = \tilde{K}_{crit}$ is estimated to be $40b$ when $\tilde{h} = 1000$, and $47b$ when $\tilde{h} = 2000$. This indicates that the idealization of the superdislocation is rather crude. A more accurate estimate of $\tilde{r}$ should be pursued in the future for the characterization of dislocation pile-ups.

Dislocations may be emitted from multiple dislocation sources. In that case, the arrangements of the dislocation cluster will be different from that in a single array pile-up. These arrangements, such as those shown by LUBARDA *et al.* (1993), would result in equivalent two-dimensional superdislocations whose effective core size, r_0, would be considerably smaller than the single array analysed here. This feature would reduce the difference between our predictions based on the idealized superdislocations and the situation in real materials. We further remark that, as long as the dislocation pile-ups are located far from the crack tip, their effects on the crack tip field should be insensitive to their arrangement.

Although the physical arguments we used in this model are generic, we calculated only a symmetric crack in the ductile layer. In the case of an interfacial crack, the crack tip would exhibit a mixed mode I and mode II field. The mathematical treatment would be more involved although still tractable. Nevertheless, we expect that the essential features of the present solution should emerge similarly. More research has to be conducted to appreciate the subtle differences between the different cases presented in Figure 2.

The present model breaks down when other competing mechanisms intervene. These include re-initiation of cleavage fracture in the brittle layer or along the interfaces away from the crack tip, considerable multiplication of dislocations in the ductile layer which could only be dealt with by continuum plasticity and crack deflection. On the other hand, when the layer thickness is below a lower limit which is of the order of atomic spacings, the continuum expressions used in this model will no longer be realistic.

In addition to the confinement due to interfaces in layered materials, other forms of confinement also exist in other material systems. For instance, grain boundaries in nanostructures may pose confinement to dislocation motion, although re-nucleation of dislocation loops in the neighboring grains is possible. Furthermore, confinement has also been observed in materials where dislocation mobility is low. HSIA and ARGON (1994) have demonstrated that, in silicon single crystals loaded at elevated

temperatures, although dislocations can emit and move away from crack tips, cleavage can still re-initiate from the blunted crack tip upon continued loading due to low dislocation mobility. The characteristics of these different forms of dislocation confinement are dependent upon specific features of the material's microstructures and micromechanisms and thus have to be analysed individually.

5. Concluding Remarks

We would like to convey in this communication that, even in very ductile FCC metals, it is still possible to achieve cleavage fracture if dislocation motion is confined. Our calculation indicates that, in a layered material with ductile layer thickness of the order of a micron, not many dislocations (less than 30) can emit from the crack tip before cleavage occurs. Therefore, the toughening resulting from the dislocation emission is rather limited. Fracture toughness of these materials would be close to the intrinsic toughness.

This analysis suggests an experimental technique to measure either the intrinsic fracture toughness of the commonly considered non-cleavable metals if interface bonding can be made strong enough, or the intrinsic toughness of interfaces, using a layered material. On the other hand, the results of this analysis alert those who are developing layered materials that the mechanical failure of these materials could be catastrophic, unless the ductile layer thickness is sufficiently large.

More experimental studies are needed to verify the predictions of the analysis. One estimate of the interfacial fracture energy Γ_i between a substrate and a metal thin film has been obtained by Bagchi *et al.* (1994). They showed that the interfacial fracture energy between copper and glass is in the range $0.3 < \Gamma_i < 0.8$ J m^{-2} for a Cu thin film of 0.44 μm. This range is indeed compatible with the work of adhesion ($W_{ad} = 0.5$ J m^{-2}) for liquid Cu on SiO_2 (Li, 1992). However, systematic experiments by varying the ductile layer thickness would help to clarify the validity regime of the present model and identify the critical conditions under which other competing mechanisms intervene.

Acknowledgements

K. J. Hsia was sponsored by the National Science Foundation through grant MSS-9209309-RIA. Z. Suo was supported by NSF through grant MSS-9258115, and by ONR through contract N00014-92-J-1808. W. Yang was supported by a visiting appointment at the University of California, Santa Barbara funded by ONR through contract N00014-93-1-0110, and by the National Natural Science Foundation of China.

References

Anderson, P. M. and Li, C. (1993) Crack-dislocation modeling of ductile-to-brittle transitions in multilayered materials. In *Thin Films: Stresses and Mechanical Properties IV* (ed. P. H. Townsend, J. Sanchez, C.-Y. Li and T. P. Weihs), p. 731. Materials Research Society Symp. Proc. 308, Pittsburgh, PA.

BAGCHI, A., LUCAS, G. E., SUO, Z. and EVANS, A. G. (1994) A new procedure for measuring the decohesion energy for thin ductile films on substrates. *J. Mater. Res.*, in press.
EVANS, A. G. and DALGLEISH, B. J. (1992) The fracture resistance of metal–ceramic interfaces. *Acta Metall. Mater.* **40,** S295–S306.
FREUND, L. B. (1987) The stability of a dislocation threading a strained layer on a substrate. *J. Appl. Mech.* **54,** 553–557.
HIRTH, J. P. and LOTHE, J. (1982) *Theory of Dislocations*, 2nd Ed. John Wiley and Sons, New York.
HSIA, K. J. and ARGON, A. S. (1994) Experimental study of the mechanisms of the brittle-to-ductile transition of cleavage fracture in Si single crystals. *Mater. Sci. Engng* **A176,** 111–119.
LANGER, J. S. (1992) Issues and opportunities in materials research. *Phys. Today* **45,** 24–31.
LI, J. G. (1992) Role of electron density of liquid metals and bandgap energy of solid ceramics on the work of adhesion and wettability of metal–ceramic systems. *Mater. Sci. Lett.* **11,** 903.
LIN, I.-H. and THOMSON, R. (1986) Cleavage, dislocation emission, and shielding for cracks under general loading. *Acta Metall* **34,** 187–206.
LUBARDA, V. A., BLUME, J. A. and NEEDLEMAN, A. (1993) An analysis of equilibrium dislocation distributions. *Acta Metall. Mater.* **41,** 625–642.
MCMEEKING, R. M. (1977) Finite deformation analysis of crack-tip opening in elastic–plastic materials and implications for fracture. *J. Mech. Phys. Solids* **25,** 357–381.
RICE, J. R., BELTZ, G. E. and SUN, Y. (1992) Peierls framework for dislocation nucleation from a crack tip. *Fundamentals of Fracture and Fatigue* (ed. A. S. ARGON), pp. 1–58. Springer, Berlin.
RICE, J. R. and THOMSON, R. (1974) Ductile versus brittle behaviour of crystals. *Phil. Mag.* **29,** 73–97.
RITCHIE, R. O., KNOT, J. F. and RICE, J. R. (1973) On the relationship between critical tensile stress and fracture toughness in mild steel. *J. Mech. Phys. Solids* **21,** 395–410.
TADA, H., PARIS, P. C. and IRWIN, G. R. (1985) *The Stress Analysis of Cracks Handbook*, 2nd Ed. Paris Productions Incorporated, St Louis, MI.
VARIAS, A. G., SUO, Z. and SHIH, C. F. (1991) Ductile failure of a constrained metal foil. *J. Mech. Phys. Solids* **39,** 963–986.

APPENDIX A. ENERGY IN A CRACKED BODY WITH DISLOCATIONS

A.1. *Single dislocation*

Consider a single dislocation located at $r = h_i$ along the slip plane. The dislocation self energy, in the presence of a semi-infinite crack, can be evaluated as the work done by dragging the dislocation against its image force along the slip plane from the crack tip to the current location h_i,

$$W_d(h_i) = \frac{\mu b^2}{4\pi(1-\nu)} \ln \frac{h_i}{r_{crack}}. \tag{A.1}$$

Here r_{crack} is the equivalent core radius to initiate a dislocation near the crack tip, and is different from the core radius of a dislocation fully embedded in a continuum. r_{crack} can be evaluated by the concept of unstable stacking energy introduced by RICE *et al.* (1992). The interaction energy between the dislocation and the crack tip K field, due to the presence of an applied K field, K_{app}, is viewed similarly as the work done by the crack tip gliding force which drives the dislocation from crack tip to its current position h_i,

$$W_K(h_i) = -\frac{K_{app}}{\sqrt{2\pi}} b\sqrt{h_i} \sin\phi \cos\frac{\phi}{2}. \tag{A.2}$$

By emission of one dislocation, an extra slice of surface emerges from the crack tip. The ledge energy is then

$$W_L(h_i) = b\gamma, \tag{A.3}$$

regardless of the value of h_i.

The pre-logarithmic factor in the self energy expression (A.1) also defines the strength of the local stress and strain field associated with the dislocation. Namely,

$$\sigma_{ij}(h_k) = \frac{\mu b}{2\pi(1-\nu)r_k}\Sigma_{ij}(\theta_k), \quad \varepsilon_{ij}(h_k) = \frac{b}{2\pi r_k}E_{ij}(\theta_k), \tag{A.4}$$

where local polar coordinates (r_k, θ_k) are centered at $r = h_k$. The forms of angular variations Σ_{ij} and E_{ij} do not depend on h_k. They are documented in the dislocation literatures, e.g. HIRTH and LOTHE (1982).

A.2. *Superdislocations*

For the two branches of dislocation pile-ups with $n/2$ dislocations in each branch located at $h_1, \ldots, h_i, \ldots, h_{n/2} = h_\phi$, the combined effect on W_K and W_L is obtained by superposition

$$W_K = -2 \times \frac{K_{app}}{\sqrt{2\pi}} b \sin\phi \cos\frac{\phi}{2} \sum_{i=1}^{n/2} \sqrt{h_i}, \quad W_L = nb\gamma. \tag{A.5}$$

They lead to (4b) and (4c). The stress and strain fields produced by one branch of the equivalent superdislocations, in a sense defined in the text, can be written as

$$\sigma_{ij} = \frac{\mu b}{2\pi(1-\nu)} \sum_{k=1}^{n/2} \frac{1}{r_k}\Sigma_{ij}(\theta_k), \quad \varepsilon_{ij} = \frac{b}{2\pi} \sum_{q=1}^{n/2} \frac{1}{r_q}E_{ij}(\theta_q), \tag{A.6}$$

in the vicinity of the dislocation cluster. The presence of a crack would not perturb those fields appreciably if the crack is relatively far away from the dislocation cluster. The self energy for one branch of the superdislocations is then

$$\begin{aligned} W_d' = \frac{1}{2}\int_V \sigma_{ij}\varepsilon_{ij}\,dV &= \frac{\mu b^2}{8\pi^2(1-\nu)} \sum_{k=1}^{n/2}\sum_{q=1}^{n/2} \int_V \frac{1}{r_k r_q}\Sigma_{ij}(\theta_k)E_{ij}(\theta_q)\,dV \\ &= \frac{\mu b^2}{4\pi(1-\nu)} \sum_{k=1}^{n/2}\sum_{q=1}^{n/2} \left(\ln\frac{h_\phi}{\Delta_{kq}} - C_{kq}\right) \end{aligned} \tag{A.7}$$

where

$$\begin{aligned} \Delta_{kq} &= r_{crack} \quad \text{if } k = q, \\ \Delta_{kq} &= |\Delta_k - \Delta_q| \quad \text{if } k \neq q. \end{aligned} \tag{A.8}$$

All of the constants C_{kq} are close to unity (HIRTH and LOTHE, 1982). The derivation toward the last step of (A.7) is based on the interaction energy formula between two dislocations k and q when Δ_{kq}/h_ϕ is much less than one. Assuming most of the h_ks are very close to h_ϕ, and the energy for the two branches is twice that for one branch given in (A.7), one finally arrives at

$$W_d = \frac{\mu(nb)^2}{8\pi(1-\nu)}(\ln(h_\phi/r_0) - C), \tag{A.9}$$

where

$$r_0 = \left(\prod_{k=1}^{n/2}\prod_{q=1}^{n/2}\Delta_{kq}\right)^{1/(n/2)^2}, \quad C = \frac{1}{(n/2)^2}\sum_{k=1}^{n/2}\sum_{q=1}^{n/2} C_{kq} \approx 1. \tag{A.10}$$

APPENDIX B. INTERACTION OF TWO DISLOCATIONS NEAR THE CRACK TIP

Consider two dislocations sitting along the same glide plane emanating from the crack tip. The leading dislocation locates at the interface of distance h_ϕ away from the crack tip. The other dislocation trails behind by a distance r_e. The force on the trailing dislocation due to the applied stress intensity factor,

$$f_K = \frac{K_{app} b}{\sqrt{8\pi(h_\phi - r_e)}} \sin\phi \cos\frac{\phi}{2}, \tag{B.1}$$

should be equal to the force exerted by the pinning dislocation at the interface

$$f_d = \frac{\mu b^2}{2\pi(1-\nu)r_e}, \tag{B.2}$$

where the Peierls–Nabarro force and the crack image force can be neglected if h_ϕ is much larger than r_e. The equilibrium spacing r_e is then derived as

$$r_e = \frac{b}{S}\left[\sqrt{1+2S\tilde{h}} - 1\right], \tag{B.3}$$

where S characterizes the strength of applied K field and is given by

$$S = \pi(1-\nu)^2 \sin^2\phi \cos^2\frac{\phi}{2} \tilde{K}_{app}^2. \tag{B.4}$$